JACS
JOURNAL OF THE AMERICAN CHEMICAL SOCIETY

Communication

pubs.acs.org/JACS

Fabricating a Reversible and Regenerable Raman-Active Substrate with a Biomolecule-Controlled DNA Nanomachine

Jing Zheng,[†] Anli Jiao,[†] Ronghua Yang,*[,†] Huimin Li,[†] Jishan Li,[†] Muling Shi,[†] Cheng Ma,[†] Ying Jiang,[†] Li Deng,[†] and Weihong Tan*[,†,‡]

[†]Molecular Science and Biomedicine Laboratory, State Key Laboratory of Chemo/Biosensing and Chemometrics, College of Chemistry and Chemical Engineering, College of Biology, Hunan University, Changsha, 410082, China

[‡]Center for Research at the Bio/Nano Interface, Department of Chemistry and Department of Physiology and Functional Genomics, Shands Cancer Center, UF Genetics Institute and McKnight Brain Institute, University of Florida, Gainesville, FL 32611, United States

Supporting Information

ABSTRACT: A DNA configuration switch is designed to fabricate a reversible and regenerable Raman-active substrate. The substrate is composed of a Au film and a hairpin-shaped DNA strand (hot-spot-generation probes, HSGPs) labeled with dye-functionalized silver nanoparticles (AgNPs). Another ssDNA that recognizes a specific trigger is used as an antenna. The HSGPs are immobilized on the Au film to draw the dye-functionalized AgNPs close to the Au surface and create an intense electromagnetic field. Hybridization of HSGP with the two arm segments of the antenna forms a triplex-stem structure to separate the dye-functionalized AgNPs from the Au surface, quenching the Raman signal. Interaction with its trigger releases the antenna from the triplex-stem structure, and the hairpin structure of the HSGP is restored, creating an effective "off–on" Raman signal switch. Nucleic acid sequences associated with the HIV-1 U5 long terminal repeat sequences and ATP are used as the triggers. The substrate shows excellent reversibility, reproducibility, and controllability of surface-enhanced Raman scattering (SERS) effects, which are significant requirements for practical SERS sensor applications.

In the past two decades, surface-enhanced Raman scattering (SERS) has become a significant technique in biomedical analysis because of its single-molecule sensitivity, molecular specificity, and insensitivity to quenching.[1−3] These distinct advantages have led to the development of a number of ingenious SERS-based biosensors to identify and detect an array of biological analytes, including small bioactive molecules,[4,5] DNA[6−8] and proteins,[9,10] and even cells.[11] To achieve maximum enhancement of the Raman signal, current research is focused on fabricating metallic substrates for generation of hot geometries (hot-spots), using either the metal surface morphology or two metal nanoparticles,[12−17] leading to enormous Raman enhancement factors on the order of 10^{14}–10^{15}. Another key requirement of any SERS substrate for practical sensor applications is reversibility and reproducibility. However, hot-spot-active substrates fabricated by traditional methods are irreversible and not regenerable, making the sensor usable only once. Fabrication of reversible and regenerable SERS-active substrates for biosensors is thus highly desirable but remains a challenge. To the best of our knowledge, no such substrate has been reported in the literature.

Herein we report a new approach for facile fabrication of a reversible and regenerable hot-spot-active substrate through the controlled organization of silver nanoparticles (AgNPs) on a Au film surface with a specially designed DNA molecular switch. Recent developments in DNA-based nanotechnology provide an attractive way to organize both metallic and semiconducting nanoparticles into periodic structures through programmable base-pairing interactions.[18,19] Using species such as DNA or antibody–antigen interactions to control the enhancement of Raman scattering, assembly of metallic nanoparticles through biomolecular recognition has been extensively studied in recent years.[6−9,20−22] Chemically, the great majority of the reported approaches rely on a dye-labeled DNA that binds to a trigger to alter the conformation of the DNA and produce the desired SERS signal. Unlike in previously reported approaches, our active substrate involves an antenna that specifically binds to a trigger and a hot-spot-generation probe (HSGP). These two moieties are assembled together through a triplex DNA structure, and a hot-spot is created by configuration conversion of the AgNPs-functionalized HSGP on the Au surface.

The fundamental concept of this approach is illustrated in Scheme 1. In our design, a central, trigger-specific single-strand (ss) DNA (in green) flanked by two arm segments (in purple) is used as an antenna, while a hairpin-shaped oligonucleotide (in blue) serves as the HSGP, with rhodamine 6G (R6G) selected as the Raman reporter. The HSGP is functionalized with AgNPs. Once the HSGP is bound with the two arm segments of the antenna via Watson–Crick and Hoogsteen base-pairing,[23,24] a "triplex-stem" structure is formed, in which the HSGP retains an "open" configuration. In this state, the R6G-functionalized AgNPs are physically separated from the Au surface, resulting in the SERS signal "off" state (low SERS effect). Conversely, upon binding with its trigger, the antenna is released from the triplex-stem structure, and the HSGP restores

Received: September 6, 2012
Published: November 28, 2012

Scheme 1. Working Principle of the DNA Nanomachine-Directed Reversible SERS-Active Substrate: (A) Structure Switch of HSGP between an Open and a Hairpin-Shaped Configuration Alternately Induced by the Trigger DNA and the Antenna, and (B) Corresponding Reversible SERS "Hot-Spot" Generation through Assembly and Disassembly of AgNPs on a Au Film Surface

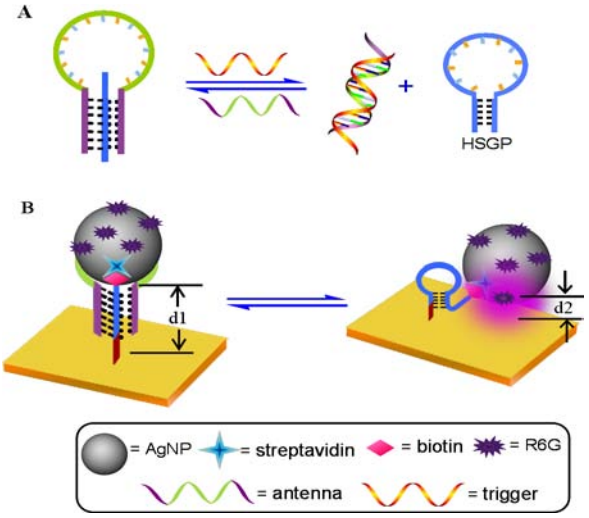

its "duplex-stem" cyclic structure, bringing the AgNPs into proximity to the Au film surface, enhancing the electromagnetic field[25,26] and producing a very large SERS signal "on" state.

For formation of the SERS hot-spot substrate, AgNPs were prepared according to a reported method.[27] Transmission electron microscopy (TEM) shows a size distribution of the formed AgNPs from 15 to 20 nm, most being 18 nm (Figure S1, Supporting Information). The UV−vis absorption spectrum shows λ_{max} = 398 nm (Figure 1, curve a), which is attributed to

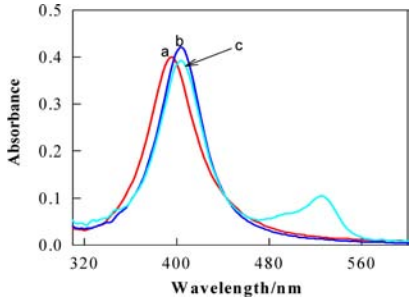

Figure 1. UV−vis absorption spectra of AgNPs (a), streptavidin-functionalized AgNPs (b), and streptavidin/R6G-functionalized AgNPs (c) in PBS.

the surface plasmon resonance of small AgNPs.[28] The AgNPs were first functionalized with streptavidin and then encoded with thiol-DNA-modified R6G (5′-thiol-TTTTT-R6G-3′). After such modification, a slight red shift of ∼7 nm was observed (curve b). When the streptavidin-functionalized AgNPs were encoded with R6G molecules, an additional absorption peak at 526 nm, the λ_{max} of R6G, clearly appeared (curve c). The surface coverage of R6G molecules on AgNPs was evaluated to be 13.5 ± 1.2 pmol/cm^2.[29] The stability of streptavidin/R6G-functionalized AgNPs was examined by measuring changes in the plasmon band absorbance under a wide range of NaCl concentrations. The functionalized AgNPs can be subjected to high ionic strengths (Figure S2).

To assemble the streptavidin/R6G-functionalized AgNPs on a Au film surface, a 36-base ssDNA (5′-biotin-CCTCC**AGAGAGAGAGAGAGAG**GGAGGAAAAAAAAAA-thiol-3′) was designed and used as HSGP. This DNA strand has a hairpin structure, including a 5-base-pair stem and a 16-base loop sequence of repeating adenine and cytosine nucleotides, as well as poly(dA)$_{10}$ at the 3′-end. Measurement of the melting temperature (T_m) indicates that this hairpin structure has moderate thermal stability, with T_m = 40 °C (Figure S3). The HSGP was then biotinylated at the 5′-end and immobilized on the Au film surface through its 3′-end thiol. The surface coverage of the HSGP on the Au surface was determined to be 10.2 ± 0.8 pmol/cm^2.[29] The Au film was subsequently treated with thiolated poly(dT)$_{10}$ to prevent other species from binding to free Au surface sites and to keep the HSGP standing fairly erect by forming an A-T duplex with the HSGP. The R6G-functionalized AgNPs were then attached to the 5′-end of the HSGP through specific streptavidin−biotin interaction.

Atomic force microscopy (AFM) was used to characterize the surface features of the Au film treated with AgNPs-functionalized HSGP and "triplex-stem" DNA, respectively. The image shows that the pure Au film prior to treatment with HSGP had a mean height of ∼10 nm, and no obvious bright spots were observed (Figure 2A), indicating that the Au surface

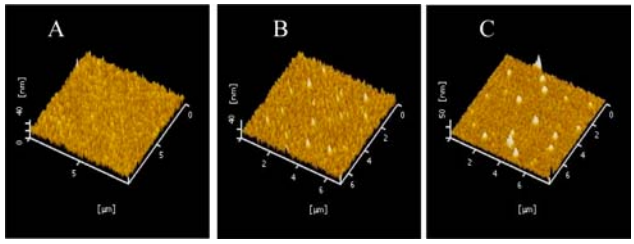

Figure 2. AFM topographic images of the bare Au film (A), the Au film bonded with streptavidin/R6G-functionalized AgNPs through HSGP (B), and as in (B), but treated with P1 to form triplex-stem cyclic DNA (C).

is enough smooth. After AgNPs were assembled on the Au film through HSGP, a few bright spots appeared in the image (Figure 2B), and the height was ∼30 nm (d2, Scheme 1B). The ∼18 nm of AgNPs, together with the 6-nm length of streptavidin plus the DNA strand, would create features with topographic heights between 25 and 35 nm. When HSGP was initially hybridized with the antenna, the open configuration of the 26-base HSGP increased the height by ∼10 nm, and AFM images appeared as many new bright spots (Figure 2C) with a mean height of 40 nm (d1, Scheme 1B).

To test the feasibility of this approach for creating SERS-active substrates, hot-spot creation was first examined using a 21-mer ssDNA (T1, 5′-ACTGCTAGA GATTTTCCACAT-3′) from the HIV-1 U5 long terminal repeat (LTR) as the trigger. The antenna (P1, 5′-TCTCTCTCATGT-GAAAATCTCTAGCAGTCTCTCTCT-3′) was designed to contain 21 bases in the middle that were identical to the complement of T1, and two arm segments to bind the loop sequence of the HSGP to form a triplex motif via T-A·T and C-G·C base triplets.[23] The sequences of the two arm segments were optimized to achieve the largest SERS signal enhancement (Figures S4 and S5). Figure 3 shows a set of SERS spectra of

dx.doi.org/10.1021/ja308875r | J. Am. Chem. Soc. 2012, 134, 19957−19960

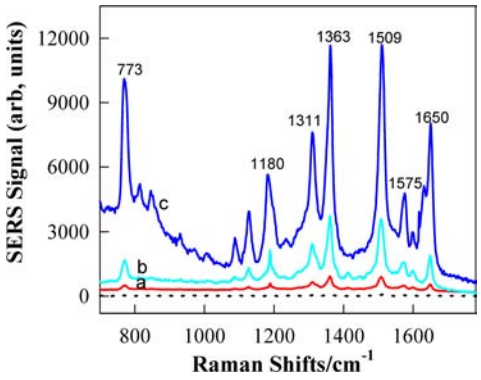

Figure 3. SERS spectra of the active substrate composed of R6G-functionalized AgNPs on Au film and P1 in PBS in the absence (a) and presence of MT1 (b) and T1 (c). Dashed line is SERS of R6G-labeled HSGP immobilized on the Au film. The concentrations of MT1 and T1 are both 1.0 μM.

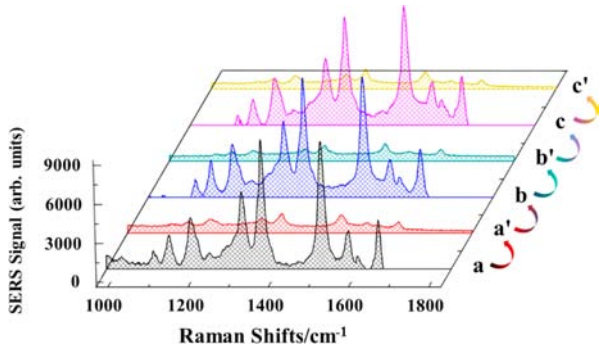

Figure 4. SERS spectra of the Au film after several repeated concentration step changes between 100 nM T1 (traces a, b, and c) and 1.0 μM P1 (traces a′, b′, and c′). The SERS spectrum was returned to its pre-exposure form by first washing with PBS three times and then immersing in the P1 solution for 2.0 h.

R6G molecules that are attached on the AgNPs upon addition of T1 in sodium phosphate buffer (PBS, pH 5.2, 20 mM NaCl and 2.5 mM $MgCl_2$). Optimization identified this pH to give the best response sensitivity (Figure S6). As expected, starting with the triplex-stem state, the SERS signals are very weak, indicating that the R6G-functionalized AgNPs are far away from the Au surface, so that no hot-spot can be generated. Hybridization of P1 with T1 releases P1 from HSGP so that the HSGP forms its initial duplex-stem cyclic structure, allowing the AgNPs to approach the Au film more closely, thereby increasing the electromagnetic field concentration in the SERS hot-spot. As a result, a strong SERS signal is observed. The spectrum characteristics are the same as those obtained for rhodamine dyes adsorbed on metallic surfaces.[30] The SERS enhancement of the most prominent Raman peak, at 1509 cm^{-1}, is estimated to be 23.6-fold upon P1 hybridization to 1.0 μM T1. In the presence of the same concentration of a single-base mismatch sequence (MT1, 5′-ACTGCTAGATATTTTC-CAC AT-3′), the SERS intensity enhancement was ~8.7-fold under the same conditions, demonstrating the specificity and selectivity of this approach and its application in selective diagnostics. A control experiment showed that measurable Raman signal when HSGP was labeled with R6G at the 5′-end and then immobilized on the Au surface (dashed line of Figure 3). According to literature methods,[32,33] an enhancement factor of $\sim 2.14 \times 10^5$ was determined (for details, see Supporting Information), indicating that no distinct Raman scattering signal could be detected without Ag-dependent electromagnetic field enhancement.[31]

Because of the strong interactions between DNA and its target, the most routinely designed generation of SERS hot-spots by DNA interaction is irreversible. In our approach, DNA hybridization and SERS hot-spot generation occur separately. Therefore, opening the hairpin structure of HSGP upon rehybridization with P1 eliminates the electromagnetic field and hot-spot-generating ability, illustrating the controlled "on−off" switching of Raman signals. To demonstrate, hybridization of P1 with T1 produces a large SERS intensity enhancement (Figure 4). Washing the Au film with PBS and subsequently immersing the Au film in the P1 solution allows the HSGP to rehybridize and restores its overall geometry to the degree required to return the SERS spectrum to its pre-exposure form. The reproducibility and reversibility of the active substrate are achieved by sequentially exposing the Au film to T1 and P1 solutions. The mean SERS intensity values of the 1509 cm^{-1} band with their confidence intervals were found to be 9070.7 ± 299.1 (n = 5, 100 nM T1) and 807.8 ± 38.2 (n = 5, 1.0 μM P1). The reversibility is related to the AgNPs size. When the hydrodynamic diameter of the AgNPs is >60 nm, the HSGP cannot return to its triplex-stem structure upon hybridization with P1 (data not shown). Nevertheless, compared to most reported methods that used DNA for the preparation of SERS substrate, our strategy—employing configuration conversion of HSGP between "open" and "duplex-stem" cyclic structures—provides advantages in terms of controllability and reproducibility.

To demonstrate the universality of this design, hot-spot creation by small-molecule interactions was studied by using adenosine triphosphate (ATP) as the trigger and the anti-ATP-binding aptamer (P2, 5′-CCTCTCTCACCTGGGGGAGTA TTGCGGAGGAAGGTCTCTCTCC-3′)[34,35] as the antenna. P2 is composed of DNA sequences for ATP and two arm segments of $d(TC)_6$ that are complementary to the central sequence of the HSGP. In the absence of ATP, the triplex-stem structure enables high SERS-quenching efficiency, but in the presence of ATP in the sample solution, significant SERS signal enhancement is observed (Figure S7). The corresponding surface features of the Au film were characterized by AFM (Figure S8). To demonstrate the potential of applying the SERS hot-spot for quantitative bioanalysis, the peak intensity at 1509 cm^{-1} was compared to the concentration of ATP (Figure S9A), revealing that the SERS signal increased with increasing ATP concentration. Initially, the peak's intensity increased ~1.3-fold when 50 nM ATP was introduced. However, with an ATP concentration of 4.0 μM, the intensity increased 19-fold, the observed saturation level (Figure S9B). The SERS intensity increases linearly with increasing ATP concentration between 25 nM and 2.0 μM (R^2 = 0.988). The detection limit of 50 nM ATP is below the dissociation constant of anti-ATP-binding ($K_d \approx 6$ μM).[32,33] This can be attributed to the occurrence of signal amplification by the ability of one or, more likely, two ATP molecules to bring about one HSGP structural change, while the SERS spectrum originates from the many tens of R6G molecules in the region of the hot-spot.

Finally, it is noteworthy that another way to create the active substrate is direct hybridization of an antenna with HSGP to form a dsDNA structure, followed by dehybridization when the antenna binds to a trigger. While this strategy offers a means of SERS hot-spot generation, it suffers from an intrinsic limitation,

dx.doi.org/10.1021/ja308875r | J. Am. Chem. Soc. 2012, 134, 19957−19960

because the HSGP is antenna sequence-dependent: in order to achieve suitable hybridization without hindering the recognition and affinity of antenna toward its trigger, optimization of the HSGP sequence length is often involved. This optimization requires preparation of several different hot-spot substrates, which means that the method would not qualify as a general approach for hot-spot generation.

In summary, a reversible and regenerable SERS hot-spot-active substrate was fabricated by employing DNA- and Raman dye-functionalized AgNPs on a Au film surface. On the basis of a configurational switch between an "open" and a "duplex-stem" cyclic DNA structure, the hot-spot effectively switches from an "off" to an "on" signal state following the action of a biological recognition event. Compared to known SERS hot-spot substrates, that created by the present approach shows excellent reversibility, reproducibility, and controllability of SERS effects, which are significant requirements for practical SERS applications. Nucleic acid sequences associated with the LTR and ATP were used to induce hot-spot generation, which, by virtue of the ability to alter the antenna sequence, is applicable to other nucleic acids, proteins, and small molecules for biomedical applications. Therefore, this hot-spot generation strategy can be considered as a universal method and opens new opportunities toward the development of more practical SERS detection systems.

■ ASSOCIATED CONTENT

Supporting Information

Experimental details including sample preparation, instrumentation, and experimental results, as well as additional information as noted in text. This material is available free of charge via the Internet at http://pubs.acs.org.

■ AUTHOR INFORMATION

Corresponding Author

yangrh@pku.edu.cn; tan@chem.ufl.edu

Notes

The authors declare no competing financial interest.

■ ACKNOWLEDGMENTS

The work was supported by NSFC (21005026 and 21135001), DFMEC (20100151120008, 20110161110006), and '973' National Key Basic Research Program (2011CB911000), and the Foundation for Innovative Research Groups of NSFC (Grant 21221003). It is also supported by grants awarded by the U.S. National Institutes of Health (GM066137, GM079359, and CA133086), by China National Instrumentation Program 2011YQ03012412, and by the special fund of Chongqing Key Laboratory.

■ REFERENCES

(1) Fleischmann, M.; Hendra, P. J.; McQuillan, A. J. *J. Phys. Lett.* **1974**, *26*, 163−166.

(2) Albrecht, M. G.; Creighton, J. A. *J. Am. Chem. Soc.* **1977**, *99*, 5215−5217.

(3) Stacy, A. M.; Van Duyne, R. P. *Chem. Phys. Lett.* **1983**, *102*, 365−370.

(4) Shafer-Peltier, K. E.; Haynes, C. L.; Glucksberg, M. R.; Van Duyne, R. P. *J. Am. Chem. Soc.* **2003**, *125*, 588−593.

(5) Kim, N. H.; Lee, S. J.; Moskovits, M. *Nano Lett.* **2010**, *10*, 4181−4185.

(6) Cao, C. Y.; Jin, R.; Mirkin, C. A. *Science* **2002**, *297*, 1536−1540.

(7) Qian, X.; Zhou, X.; Nie, S. M. *J. Am. Chem. Soc.* **2008**, *130*, 14934−14935.

(8) Kang, T.; Yoo, S. M.; Yoon, I.; Lee, S. Y.; Kim, B. *Nano Lett.* **2010**, *10*, 1189−1193.

(9) Cao, Y. C.; Jin, R. C.; Nam, J. M.; Thaxton, C. S.; Mirkin, C. A. *J. Am. Chem. Soc.* **2003**, *125*, 14676−14677.

(10) Bonham, A. J.; Btaun, G.; Pavel, I.; Moskovits, M.; Reich, N. O. C. A. *J. Am. Chem. Soc.* **2007**, *129*, 14572−14573.

(11) Kneipp, J.; Kneipp, H.; Rice, W. I.; Kneipp, K. *Anal. Chem.* **2005**, *77*, 2381−2385.

(12) Lee, S. J.; Morrill, A. R.; Moskovits, M. *J. Am. Chem. Soc.* **2006**, *128*, 2200−2201.

(13) Kang, T.; Yoon, I.; Jeon, K. S.; Choi, W.; Lee, Y.; Seo, K.; Yoo, Y.; Park, Q. H.; Ihee, H.; Suh, Y. D.; Kim, B. *J. Phys. Chem. C* **2009**, *113*, 7492−7496.

(14) Shegai, T.; Vaskevich, A.; Rubinstein, I.; Haran, G. *J. Am. Chem. Soc.* **2009**, *131*, 14390−14398.

(15) Li, J. F.; Huang, Y. F.; Ding, Y.; Yang, Z. L.; Li, S. B.; Zhou, X. S.; Fan, F. R.; Zhang, W.; Zhou, Z. Y.; Wu, D. Y.; Ren, B.; Wang, Z. L.; Tian, Z. Q. *Nature* **2010**, *464*, 392−395.

(16) Rycenga, M.; Xia, X. H.; Moran, C. H.; Zhou, F.; Qin, D.; Li, Z. Y.; Xia, Y. A. *Angew. Chem., Int. Ed.* **2011**, *50*, 5473−5477.

(17) Wei, K. K.; Xiang, S. Z.; Malini, O. *Anal. Chem.* **2012**, *84*, 908−916.

(18) Aldaye, F. A.; Palmer, A. L.; Sleiman, H. F. *Science* **2008**, *321*, 1795−1799.

(19) Sharma, J.; Chhabra, R.; Cheng, A.; Brownel, J.; Liu, Y.; Yan, H. *Science* **2009**, *323*, 112−116.

(20) Graham, D.; Thompson, D. G.; Ewen Smith, T. W.; Faulds, K. *Nat. Nanotechnol.* **2008**, *3*, 548−551.

(21) Kim, N. H.; Lee, S. J.; Moskovits, M. *Adv. Mater.* **2011**, *23*, 4152−4156.

(22) Zhang, Z. L.; Wen, Y. Q.; Ma, Y.; Luo, J.; Zhang, X. Y.; Jiang, L.; Song, Y. L. *Appl. Phys. Lett.* **2011**, *98*, 133704.

(23) Salunkhe, M.; Wu, T. F.; Letsinger, R. L. *J. Am. Chem. Soc.* **1992**, *114*, 8768−8772.

(24) Zheng, J.; Li, J. S.; Jiang, Y.; Jin, J. Y.; Wang, K. M.; Yang, R. H.; Tan, W. H. *Anal. Chem.* **2011**, *83*, 6586−6592.

(25) Xu, H.; Aizpurua, J.; Käll, M.; Apell, P. *Phys. Rev. E* **2000**, *62*, 4318−4324.

(26) Moskovits, M.; Tay, L.; Yang, J.; Haslett, T. *Top. Appl. Phys.* **2002**, *82*, 215.

(27) Lee, P.; Meisel, D. J. *J. Phys. Chem.* **1982**, *86*, 3391−3395.

(28) Kelly, K. L.; Coronado, E.; Zhao, L. L.; Schatz, G. C. *J. Phys. Chem. B* **2003**, *107*, 668−677.

(29) Demers, L. M.; Mirkin, C. A.; Mucic, R. C.; Reynolds, R. A.; Letsinger, R. L.; Elghanian, R.; Viswanadham, G. *Anal. Chem.* **2000**, *72*, 5535−5541. For details, see Supporting Information.

(30) Jiang, J.; Bosnick, K.; Maillard, M.; Brus, L. *J. Phys. Chem. B* **2003**, *107*, 9964−9972.

(31) Cao, Y. C.; Jin, R.; Mirkin, C. A. *Science* **2002**, *297*, 1536−1540.

(32) Braun, G.; Lee, S. J.; Dante, M.; Nguyen, T. Q.; Moskovits, M.; Reich, N. *J. Am. Chem. Soc.* **2007**, *129*, 6378−6379.

(33) Yan, J.; Su, S.; He, S. J.; He, Y.; Zhao, B.; Wang, D. F.; Zhang, H. L.; Huang, Q.; Song, S. P.; Fan, C. H. *Anal. Chem.* **2012**, *84*, 9139−9145.

(34) Huizenga, D. E.; Szostak, J. W. *Biochemistry* **1995**, *34*, 656−665.

(35) Urata, H.; Nomura, K.; Wada, S.; Akagi, M. *Biochem. Biophys. Res. Commun.* **2007**, *360*, 459−463.